ECOGRAPHY

Research

Disentangling elevational richness: a multi-scale hierarchical Bayesian occupancy model of Colorado ant communities

Tim M. Szewczyk and Christy M. McCain

T. M. Szewczyk (http://orcid.org/0000-0002-5268-6708) ✉ (timothy.szewczyk@unh.edu), Dept of Natural Resources and the Environment, Univ. of New Hampshire, NH, USA, and Dept of Computer Science, Univ. of New Hampshire, NH, USA. – C. M. McCain (http://orcid.org/0000-0002-6416-0703), Dept of Ecology and Evolutionary Biology, Univ. of Colorado, Boulder, CO, USA, and Univ. of Colorado Museum of Natural History, Univ. of Colorado, Boulder, CO, USA.

Ecography
42: 977–988, 2019
doi: 10.1111/ecog.04115

Subject Editor: John-Arvid Grytnes
Editor-in-Chief: Miguel Araújo
Accepted 19 November 2018

Understanding the forces that shape the distribution of biodiversity across spatial scales is central in ecology and critical to effective conservation. To assess effects of possible richness drivers, we sampled ant communities on four elevational transects across two mountain ranges in Colorado, USA, with seven or eight sites on each transect and twenty repeatedly sampled pitfall trap pairs at each site each for a total of 90 d. With a multi-scale hierarchical Bayesian community occupancy model, we simultaneously evaluated the effects of temperature, productivity, area, habitat diversity, vegetation structure, and temperature variability on ant richness at two spatial scales, quantifying detection error and genus-level phylogenetic effects. We fit the model with data from one mountain range and tested predictive ability with data from the other mountain range. In total, we detected 105 ant species, and richness peaked at intermediate elevations on each transect. Species-specific thermal preferences drove richness at each elevation with marginal effects of site-scale productivity. Trap-scale richness was primarily influenced by elevation-scale variables along with a negative impact of canopy cover. Soil diversity had a marginal negative effect while daily temperature variation had a marginal positive effect. We detected no impact of area, land cover diversity, trap-scale productivity, or tree density. While phylogenetic relationships among genera had little influence, congeners tended to respond similarly. The hierarchical model, trained on data from the first mountain range, predicted the trends on the second mountain range better than multiple regression, reducing root mean squared error up to 65%. Compared to a more standard approach, this modeling framework better predicts patterns on a novel mountain range and provides a nuanced, detailed evaluation of ant communities at two spatial scales.

Keywords: diversity, elevational gradient, Formicidae, community, predictive model

NORDIC SOCIETY OIKOS

www.ecography.org

Introduction

Understanding the distribution of biodiversity has been a longstanding drive in ecology and is critical to effective conservation. Many explanations for the observed patterns have been proposed (Pianka 1966, Rosenzweig 1995, Mittelbach et al. 2007), and building evidence points toward several drivers jointly shaping richness in complex ways. Global elevation analyses have identified current climate as a key driver, though effects may be indirect via productivity, or moderated by variables like area (McCain 2007a, 2009, 2010, Beck et al. 2012, Szewczyk and McCain 2016). Some hypothesized drivers, including habitat complexity and biotic interactions, remain insufficiently evaluated.

Robust and generalized inference is made difficult by the complex suite of potentially interacting hypothesized processes (Pianka 1966, Rosenzweig 1995, Lomolino 2001, Currie et al. 2004, Mittelbach et al. 2007, Laiolo et al. 2018). These richness drivers may be causally linked or exert influence through multiple mechanisms (Rosenzweig 1995, Beck et al. 2012) with effects contingent on spatial grain and extent (Hortal et al. 2010, McGill 2010). Along a given elevational gradient, a taxon's empirical richness pattern is the emergent product of any number of processes at the community- and species-scale, including deterministic effects of underlying local and regional drivers, evolutionary history, and inherent stochasticity. Additionally, the true richness may be obscured by imperfect detection, which varies among species (MacKenzie et al. 2002, Kéry and Royle 2008). The integration of local and regional effects is natural to hierarchical models, and Bayesian models in particular are amenable to incorporating data at several spatial scales, accounting for multiple sources of uncertainty, and including nuanced structural relationships (Dennis 1996, Ellison 2004, Kéry and Royle 2008, Beck et al. 2012).

The large spatiotemporal scales of many relevant processes also make generalized inference challenging. Mountains, encompassing a broad range of conditions on every continent, provide compact, naturally 'replicated' elevational gradients to assess the relative influence of hypothesized richness drivers (Rahbek 1995, McCain 2007b). Though logistical realities often limit elevational richness studies to one transect, those studies with replicated elevational transects confirm that similar conditions can generate quite disparate richness patterns (Grytnes 2003, Sanders et al. 2003). This suggests either the exclusion of relevant variables or a large degree of stochasticity and process error, and emphasizes the necessity of replication across multiple transects or across multiple years.

The vast majority of animals are insects, though a disproportionate amount of work has focused on vertebrates (Hortal et al. 2010, Beck et al. 2012). Here, we focus on ants, a particularly useful insect clade. Diverse in nearly all terrestrial systems, they have large ecological impacts and are well-described. Like most taxa, ants are most diverse in the tropics (Moreau and Bell 2013). Across elevations, richness is variable; the best-sampled transects often show mid-elevation richness peaks, though decreases and low-elevation plateaus also occur (Szewczyk and McCain 2016, and references therein, Longino and Branstetter 2018).

Available energy has often been suggested to drive richness, both directly and indirectly (Pianka 1966, Fisher 1996, Kaspari et al. 2000, 2004, Hawkins et al. 2003, Currie et al. 2004, Evans et al. 2005, Mittelbach et al. 2007, Sanders et al. 2007, Longino and Colwell 2011). Warmer temperatures may increase metabolic rates, driving increases in both ecological and evolutionary processes (Allen et al. 2002). In ectothermic taxa such as ants, temperature could increase foraging times or hasten larval development, allowing more rapid colony growth (Hölldobler and Wilson 1990, Kaspari et al. 2000, 2004) and perhaps accelerating specialization and diversification over evolutionary time. Indirectly, warmer temperatures often lead to higher productivity, which may increase speciation rates, decrease extinction rates, or allow more individuals to coexist (Currie et al. 2004, Harrison and Grace 2007). Productivity may be relevant broadly as the average productivity or locally as microsite variation (Harrison and Grace 2007, Hortal et al. 2010, Munyai and Foord 2012). Though monotonic increases in richness with temperature have been observed in ants (Sanders et al. 2007), as predicted by direct effects of temperature, ants in aggregate are inconsistent with such a relationship, often exhibiting highest richness at intermediate elevations (Olson 1994, Samson et al. 1997, Botes et al. 2006, Sabu et al. 2008, Munyai and Foord 2012, Szewczyk and McCain 2016, Longino and Branstetter 2018). A lack of global high-resolution data has prevented a comprehensive evaluation of thermal effects via productivity (McCain 2010), though ant elevational richness is broadly consistent with productivity predictions since richness is often highest in the warmest, wettest elevations (McCain 2007a, Szewczyk and McCain 2016, but see: Kaspari et al. 2000, 2004, Sanders et al. 2003, 2007). Thermal stability may also shape richness (Pianka 1966, Stein et al. 2014), as tolerance to high annual climatic variation allows species to occupy a broader set of conditions in space, resulting in larger range sizes (Janzen 1967, Stevens 1992).

Aside from climate, several other aspects of the physical environment likely affect richness. Larger areas with similar conditions allow larger ranges, which in turn decrease extinction rates and increase speciation rates (Rosenzweig 1995). More immediately, larger areas are more likely to encompass more habitats and consequently more species (Terborgh 1973, Rosenzweig 1995). Habitat heterogeneity and complexity have many definitions (Stein et al. 2014), and so we distinguish 'habitat heterogeneity' as diversity of broad habitat types, and 'habitat complexity' as local vegetation structure. Habitat heterogeneity affects species diversity given any degree of specialization, but does not follow a consistent elevational pattern. The relevant habitat complexity axes depend on the focal taxon (Rosenzweig 1995, Stein et al. 2014), and for ants, proposed variables include litter depth (Bharti et al. 2013), undergrowth structure (Lassau and Hochuli 2004, Pacheco and Vasconcelos 2012), tree density (Queiroz and Ribas 2016), and canopy cover (Lassau and Hochuli 2004, Pacheco and Vasconcelos 2012, Queiroz and

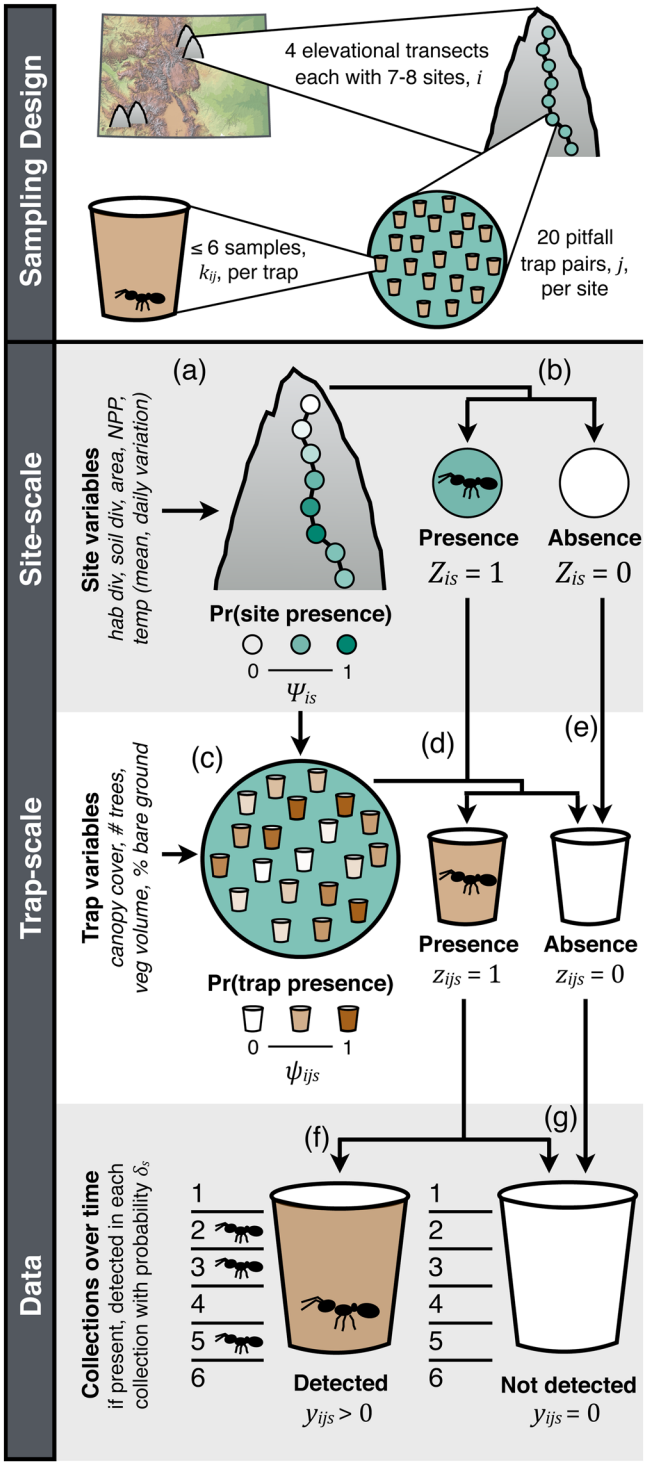

Figure 1. Sampling design and model spatial structure. Four elevational gradients in Colorado were sampled, with two in the San Juans and two in the Front Range. Each gradient consisted of 7–8 sites, i, separated by ~250 m in elevation. At each site, 20 pairs of pitfall traps, j, collected insects. Traps were set for 90 d during the summer with up to 6 collections, k_{ij}, per trap. Each ant species, s, was detected $0 - k_{ij}$ times at each trap, with y_{ijs} total detections at a trap. (a) The probability that species s occurs at site i, Ψ_{is} (darker = higher probability of occurrence), is driven by its response to the variables within that elevational band (site variables: land cover diversity, soil type diversity, area, NPP, mean annual temperature, daily temperature variation). (b) The presence, $Z_{is} = 1$, or absence, $Z_{is} = 0$, of species s at site i depends on Ψ_{is}. That is, in each iteration of the model, $Z_{is} = 1$ with probability Ψ_{is}. (c) The probability that species s occurs at trap j of site i, ψ_{ijs} (darker = higher probability of occurrence), is driven by its response to the conditions at the trap (trap variables: canopy cover, number of trees, understory vegetation volume, percent bare ground), but also by the overall probability of occurring at the site, Ψ_{is}. (d) If present at site i, species s is present at trap j, $z_{ijs} = 1$, with probability ψ_{ijs}. (e) If absent at site i, species s is absent at all traps within that site. (f) If present at trap j, species s is detected with probability δ_s in each collection of the trap, with a total of y_{ijs} detections. (g) If not detected at a trap, $y_{ijs} = 0$, species s could either be present but undetected, or truly absent.

Ribas 2016). While area is partly consistent as a driver of ant elevational richness (Sanders 2002, Bishop et al. 2014, Szewczyk and McCain 2016), even the direction of any effect of habitat complexity on ant richness is unclear, with decreases attributed to less efficient movement or chemical signaling (Lassau and Hochuli 2004), and increases to more varied niche space (Andersen 1986, Pacheco and Vasconcelos 2012). Species richness is determined by the overlap of species' geographic distributions, which are influenced by the taxon's evolutionary history (Moreau and Bell 2013). The climate during a major diversification may have long-lasting effects, with the ancestral niche echoing through descendent species (Webb et al. 2002, Wiens and Donoghue 2004). Current ant richness patterns may reflect the warm climate of the Cretaceous Neotropics where many major clades arose (Brady et al. 2006, Moreau and Bell 2013). While thermal tolerances certainly vary among species, the historical preference for warmth may be evident at deeper taxonomic levels (Wiens and Donoghue 2004). Further, accounting for the phylogenetic non-independence of species allows more robust inference of overall aggregate effects.

In this study, we evaluate hypothesized richness drivers along four elevational transects across two mountain ranges using replicated productivity, habitat heterogeneity, habitat complexity, climate, and species richness data. While accounting for detection error and potential phylogenetic effects, we incorporate the intricacies of the sampling design and the possibility of multiple factors acting at different spatial scales. We use data from one mountain range to parameterize this community-level hierarchical Bayesian occupancy model, reserving the other mountain range as a novel, out-of-sample dataset to test its predictive ability.

Methods

Sampling

We sampled four elevational transects (Fig. 1) in Colorado, USA during the summers of 2010–2012 with eight sites separated by ~250 m elevationally on each transect, and

with two transects in the San Juan Range (*SJ*-1: 1796–3508 m; *SJ*-2: 1493–3517 m) and two in the Front Range (*FR*-1: 1728–3640 m; *FR*-2: 1811–3659 m). The mountains of Colorado comprise a large portion of the Southern Rocky Mountains. The San Juan Range is a massif found in the southwestern corner of the state, while the Front Range runs primarily north-south through north central Colorado. The San Juan Range extends from desert shrubland at ~1400 m through pinyon-juniper, Gambel's oak, Douglas fir, and Engelmann spruce forests to the alpine as high as 4365m. The Front Range extends from semi-arid grassland at ~1600 m through Ponderosa pine, Douglas fir, Engelmann spruce forests, and the alpine to 4352 m (Gregg 1963). Each site was sampled for one summer (i.e. 90 d). At each site, twenty sampling plots, separated by 70 m, were distributed among meadow, forest, rocky, and riparian habitats in proportion to the habitat abundance as estimated by satellite images. At each plot, two pitfall traps were placed 3m east and west of a center point. Each trap consisted of two nested plastic cups (d: 9 cm, h: 12 cm) with propylene glycol as a killing agent and preservative. Due to non-independence, the samples from each pair of pitfall traps were pooled, leaving twenty independent samples at each site; hereafter, each pair of traps is referred to as a pitfall trap. Pitfall traps were collected up to six times throughout the 90-d sampling period, with a median of four collections. The traps from several FR sites, though set for the full period, were collected less regularly (Supplementary material Appendix 1 Table A1). Hence, we parameterized the model with the SJ transects, reserving the FR transects as novel datasets to test the model as an out-of-sample validation. We excluded three sites from this analysis due to excessive disturbance by mammals, mostly bears and marmots, with one excluded site each on *SJ*-1, *SJ*-2, and *FR*-2 (Supplementary material Appendix 1 Table A1). With four transects across two mountain ranges, 7–8 sites per transect, 40 pitfall traps per site, and 90 sampling days per pitfall, this is the most exhaustive elevational ant richness study in the Rocky Mountains to date.

Pitfall samples were cleaned and sorted in the lab. Ants were separated, transferred to 70% ethanol, and identified to species or morphospecies using appropriate keys (Gregg 1963, Mackay and Mackay 2002) and comparison to museum specimens. Specimens are stored in 70% ethanol in the Univ. of Colorado Museum entomology collections.

Understory vegetation ground coverage (< 1 m) was estimated within a 1 m radius of the center point of each sampling plot for grass, forb, shrub, cactus, and bare ground using Braun–Blauquet coverage classes (+: < 1%; 1: 1–5%; 2: 5–25%; 3: 25–50%; 4: 50–75%; 5: > 75%). At 3 m north, south, east, and west of the center as well as center, we measured understory vegetation height (< 1 m) and recorded canopy coverage with a densiometer facing the plot center. Within a 5 m radius, the number of trees was counted and the diameter at breast height measured for trees > 3 cm. These surveys were performed at the start, middle, and end of the summer sampling season.

Despite thorough sampling and including detection and sampling error, we also calculated richness estimators using EstimateS 9.1.0 (Colwell 2013). We calculated ICE and Fisher's α using the number of instances of a species at a trap instead of abundance, due to the social nature of ant foraging and hence pitfall captures (Bestelmeyer et al. 2000). In addition, we calculated species accumulation curves with the R package 'vegan', and rarefaction and extrapolation curves with the R package 'iNEXT' (Chao and Jost 2012, Colwell et al. 2012, Chao et al. 2014).

Hypothesized drivers

At the site-scale, we evaluated climate, productivity, habitat heterogeneity, and area as drivers. We used mean annual temperature (PRISM 30-yr normals; resolution: 800 m^2; 1981–2010) and mean diurnal temperature range (WorldClim; resolution: ~1 km^2; 1950–2000), calculating the mean of each variable in each 100 m elevational band. Temperature and precipitation were highly correlated, so we did not include precipitation due to its slightly higher correlations with other variables (e.g. precipitation-area: r=–0.91; precipitation-diurnal temperature range: r=–0.81). To test site-scale productivity, we calculated mean net primary productivity (NPP) in each 100 m elevational band using MODIS estimates (MOD17A3; resolution: ~1 km^2; 2000–2013). We estimated habitat heterogeneity at the site-scale as land cover diversity (National Land Cover Database 2011; excluding perennial ice/snow, open water, developed high and medium intensity; resolution: 30 m) and as soil type diversity (USDA: STATSGO2; resolution: rasterized to 30 m). For each, we calculated Shannon's diversity index within each 100 m elevational band. We calculated area from the USGS NED dataset (resolution: ~30 m^2; accessed 2016) using the Real Surface Area SAGA 2.1.4 algorithm, summing the surface area within each 100 m elevational band.

At the trap-scale, we evaluated local productivity and habitat complexity as drivers. For productivity, we used vegetation measurements at each sampling plot, estimating the vegetation biomass as the mean across visits of the vegetation volume, and the proportion of bare ground as the mean across visits. We estimated habitat complexity as the maximum canopy coverage recorded during the summer and as the number of trees in each sampling plot.

For GIS-based datasets (e.g. climate, area), transect boundaries were determined by creating a 30 km buffer around a line connecting the sites of each transect, then clipping using the 8-digit hydrologic unit watershed boundaries (USDA/NRCS). Transect boundaries are thus defined by major ridgelines within a 30 km radius of the transect lines (McCain 2007b, Szewczyk and McCain 2016). All GIS analyses were performed in QGIS 2.14.0 and R 3.2.0 with the 'vegan' and 'raster' packages.

A full species-level phylogeny is not available for Colorado ants. Instead, we evaluated the influence of genus-level relationships (Smith 2015) using a genus phylogeny

(Kumar et al. 2017) pruned to inlcude only genera occurring within Colorado with the 'ape' package in R 3.5.1 (Supplementary material Appendix 1 Fig. A1).

Model structure

We developed a community-level hierarchical Bayesian occupancy model to evaluate the influence of hypothesized richness drivers simultaneously while accounting for possible phylogenetic covariance, differences in the spatial scale of the driver's effects, and imperfect detection (MacKenzie et al. 2002, Nichols et al. 2008). The full model includes a data submodel describing the observation process, a trap-scale ecological submodel describing local processes, a site-scale ecological submodel describing regional processes, and a parameter submodel describing how species-specific responses are distributed among ant species. The observed richness pattern can be considered one realization from multiple underlying probabilistic ecological and observational processes (Fig. 1; Supplementary material Appendix 2).

Occupancy & detection

The probability that species s occurs at trap j of site i depends on the conditions at the site-scale, e.g. temperature (Fig. 1a), and at the trap-scale, e.g. canopy cover (Fig. 1c; Nichols et al. 2008, Kroll et al. 2015). However, a species may not be detected at a trap or site even though it is present (Fig. 1g). In the data submodel, we use the number of detections of each species at each trap, y_{ijs}, to estimate a species-specific detection probability, δ_s, as well as the true, latent occupancy state at each site Z_{is} (Fig. 1b) and trap z_{ijs} (Fig. 1d–e), where 1 represents presence and 0 absence. Thus, species s has some probability of occurring at site i, $\Psi_{is} = \Pr(Z_{is} = 1)$, some probability of occurring at trap j if present at site i, $\psi_{ijs} = \Pr(z_{ijs} = 1 \mid Z_{is} = 1)$, and some probability of being detected if present at trap j, $\delta_s = \Pr(y_{ijs} > 0 \mid z_{ijs} = 1)$. The number of detections of species s at trap j (Fig. 1f–g) is $y_{ijs} \sim \text{Binomial}(\delta_s z_{ijs}, k_{ij})$, where k_{ij} is the number of collections at trap j.

Site-scale drivers

In the site-scale process submodel, the probability that species s occurs at site i is driven by its response to the site-scale conditions (Fig. 1a):

$$\text{logit}\left(\Psi_{is}\right) = \beta_1 HabDiv_i + \beta_2 SoilDiv_i + \beta_3 \log\left(Area\right)_i + b_{1s}\left|\omega_s - Temp_i\right| + b_{2s} NPP_i + b_{3s} DTR_i + a_{1s}$$

where β_x is a community-level response, b_{xs} is a species-specific response, and a_{1s} is the species-specific intercept. Note that we do not assume monotonic responses to temperature. Rather, we estimate each species' thermal optimum (ω_s) and a parameter describing thermal breadth (b_{1s}), a more biologically realistic approach similar to mid-point attractor models (Colwell et al. 2016). Area and habitat heterogeneity theoretically affect richness more directly rather than each species individually (Pianka 1966, Rosenzweig 1995), and we estimate only aggregate responses for these three variables rather than species-specific responses. The site presence for a species (Fig. 1b) is then $Z_{is} \sim \text{Bernoulli}(\Psi_{is})$.

Trap-scale drivers

In the trap-scale process submodel, the probability that species s occurs at trap j of site i is driven by its response to the trap-scale conditions and the probability of presence at site i (Fig. 1c):

$$\text{logit}\left(\psi_{ijs}\right) = \rho\,\text{logit}\left(\Psi_{is}\right) + b_{4s} CanopyCover_{ij} + b_{5s} nTrees_{ij} + b_{6s} VegBiomass_{ij} + b_{8s} BareGround_{ij} + a_{2s}$$

where ρ scales the effect of the site-scale probability and a_{2s} is the species-specific intercept. Thus, the probability of site occurrence impacts the probability of trap occurrence if $\rho > 0$. Trap presence (Fig. 1d–e) is $z_{ijs} \sim \text{Bernoulli}(\psi_{ijs} Z_{is})$ with trap presence contingent upon site presence. For each species, therefore, the model estimates slopes b_{xs}, a thermal optimum ω_s, occupancy probabilities ψ_{ijs} and Ψ_{is}, occupancy states z_{ijs} and Z_{is}, and a detection probability δ_s.

Phylogenetic effects

In the parameter submodel, we allow two levels of phylogenetic correlation among species. The species-level responses, b_{xs}, ω_s, and a_{xs}, are distributed about latent genus-level means, B_{xg}, such that $b_{xs} \sim \text{Normal}(B_{xg}, e_x)$ with one standard deviation term for each variable, e_x, describing variation in congener responses. This method incorporates supported genus-level relationships in the absence of a comprehensive species-level phylogeny (Hadfield and Nakagawa 2010). The genus-level means are distributed about aggregate means that represent the overall response, such that $B_{xg} \sim \text{mvNormal}(\beta_x, \lambda_x \Sigma_{phylo} + I(1 - \lambda_x))$. Here, β_x is the aggregate response, I is an identity matrix, Σ_{phylo} is the covariance matrix calculated from the phylogeny, and λ_x is Pagel's λ, where $\lambda = 1$ indicates perfect phylogenetic covariance and $\lambda = 0$ indicates none (Pagel 1999). Thus, for each variable, we estimate the overall aggregate response β_x, genus-specific responses B_{xg}, species-specific responses b_{xs}, variation among congeners e_x, and phylogenetic covariance among genera λ_x.

Uninformative priors were used for slopes; weakly informative priors restricted some parameters to allowable values (e.g. λ_x limited to 0–1; Supplementary material Appendix 1 Table A2). All models were fit in R 3.5.1 using JAGS 4.0.1 and the 'R2Jags' package. Highest probability density intervals (HPDIs) were calculated using the 'coda' package. Each model was run with 8 chains of 100 000 iterations each, with the first half discarded as burn-in and every 200th iteration retained for the posterior distribution to avoid autocorrelation. The model code is available in Supplementary material Appendix 2.

Model comparison

After fitting the model using the two San Juan transects, we tested the ability of the model to predict richness along the two Front Range transects, representing true out-of-sample

evaluation. To generate candidate variable sets, we used a backwards stepwise method, given the prohibitive number of possible models and computing time. Beginning with the full model (m_{full}), we successively removed the variable whose β posterior distribution most overlapped zero, fitting the smaller model and repeating until the 95% HPDIs excluded 0 for all β. This generated our set of candidate models for comparison.

To compare candidate models, we tested each model's predictive accuracy with the novel *FR*-1 and *FR*-2 transects in two ways (Hooten and Hobbs 2015). First, we restricted predictions to species occurring in both mountain ranges, using species-level estimates (i.e. b_{xs}) with Front Range covariates to predict the Front Range elevational richness of the mutual community (FR_{shared}). Using full posterior distributions, we calculated $\Pr(y_{ijs} \mid \delta_s, z_{ijs})$ for each iteration. The best model based on these out-of-sample predictions (m_{opt}) was chosen using the log pointwise posterior density (Hooten and Hobbs 2015). Second, we repeated this using all Front Range species (FR_{all}) including species not used to fit the model. This represents a community with a novel set of species in a novel mountain range. From aggregate parameter estimates (i.e. β_x), we drew genus- and species-level parameters from the associated distributions. To account for the additional stochasticity in the phylogenetic hierarchy, we drew ten sets of parameters for each iteration, resulting in 10 000 predicted richness curves.

Finally, we compared the predictive ability of our model with that of a multiple linear regression using site-scale interpolated richness and site-scale variables. We fit all possible models with San Juan data, using AIC_c to select the best model (m_{lm}). We then predicted site-scale interpolated richness using the parameterized model and Front Range covariates. Thus, all model comparisons were performed using transects *FR*-1 and *FR*-2 as novel, out-of-sample data.

Data deposition

Data available from the Dryad Digital Repository: <https://doi.org/10.5061/dryad.rt679ng> (Szewczyk and McCain 2018).

Results

We detected 105 species (SJ: 92; FR: 76), with 8130 species-instances and 135 039 workers in 1600 collections after eliminating disturbances. Richness peaked at intermediate elevations on all transects (Fig. 2), though the elevation varied somewhat (*SJ*-1: 2200 m, *SJ*-2: 2300 m, *FR*-1: 1900 m, *FR*-2: 2200 m). Observed richness, ICE, and Fisher's α were highly correlated ($r > 0.97$; Fig. 2) and species accumulation and extrapolation curves generally appeared to approach asymptotes (Supplementary material Appendix 1 Fig. A2), confirming adequate sampling effort for richness pattern detection. The optimal model determined by out-of-sample predictive ability, m_{opt}, included just mean annual temperature and trap-scale canopy cover (Fig. 3, Supplementary material Appendix 1 Table A3).

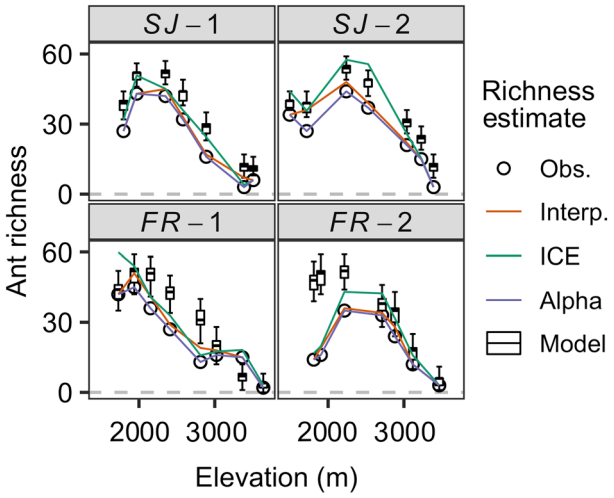

Figure 2. All estimators for site-scale richness were highly correlated with each other and with observed and modeled ant richness. On all transects, richness peaks at intermediate elevations. Shown are the site-scale estimates on each transect for observed richness (circles), interpolated richness (orange line), ICE (green line), and Fisher's α (purple line). The boxplots show estimated richness based on the posterior distribution for occupancy states in m_{full} (i.e. Z_{is}; thick bar: median; box: 50% highest posterior density interval (HPDI); capped line ranges: 95% HPDI). San Juan boxes (SJ: top row) show values estimated from the model; Front Range boxes (FR: bottom row) show values predicted by the fitted model.

Site-scale drivers

At the site-scale, temperature was supported as a combination of species-specific thermal optimum and breadth (Fig. 3; Supplementary material Appendix 1 Table A3). The overall aggregate optimum occurred at mean annual temperatures around 9.4°C, corresponding to ~1950 m in the San Juans and ~1850 m in the Front Range, with a strong decline in occurrence probability away from the optimum, indicated by the strongly negative thermal breadth. Nearly all genus-level thermal optima were in the lower half of each gradient, as were those of most species, though several showed a clear preference for colder temperatures (Supplementary material Appendix 1 Fig. A3). No other site-scale variables were included in m_{opt}, though m_{full} estimated a positive effect of NPP, a negative effect of soil type diversity, and a marginal positive effect of daily temperature range. The responses for area and land cover diversity were not distinguishable from zero (Fig 3; Supplementary material Appendix 1 Table A3).

Trap-scale drivers

At the trap-scale, only canopy cover was supported, with a tendency for decreased richness where canopy cover was higher. Tree density, understory vegetation biomass, and bare ground coverage had no overall effect on richness (Fig. 3; Supplementary material Appendix 1 Table A3).

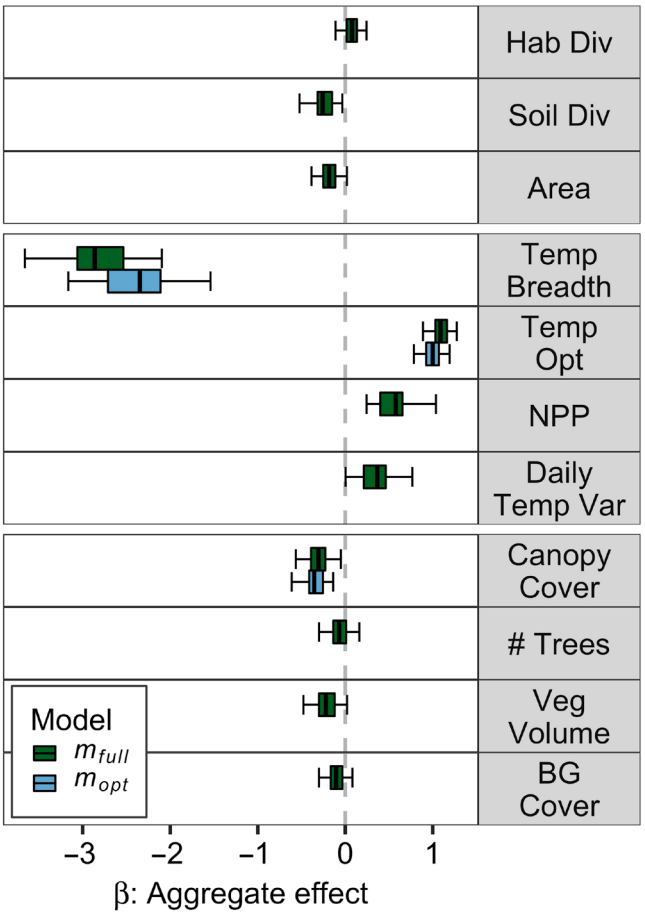

Figure 3. Parameter posterior distribution summaries for m_{full} and m_{opt}. Boxes show aggregate (i.e. β) posterior distributions (thick bar: median; box: 50% highest posterior density interval (HPDI); capped line ranges: 95% HPDI) for the full model (m_{full}: green) and the optimal model based on predictions for the novel Front Range transects (m_{opt}: blue). All covariates were centered and scaled to a standard normal distribution.

Phylogenetic effects

The genus-level phylogeny had minimal detectable impact, indicated by the highly uncertain estimates of λ (Supplementary material Appendix 1 Table A4 and Fig. A4a). However, congeners largely responded similarly; the median estimate for intrageneric standard deviation, e_x, was less than one for all variables (Supplementary material Appendix 1 Fig. A4b). Congeners varied more in their thermal breadth than in response to any other variable, though uncertainty was also higher.

Detectability

The distribution of species' detection probabilities peaked at ~40% (Supplementary material Appendix 1 Fig. A5), corresponding to a species detected in 2 of 5 pitfall collections when present, assuming 2–3 week trapping bouts. Further, the distribution is skewed right, indicating a greater number of low-detectability species and relatively few high-detectability species. The shape of this distribution held constant across candidate models (Supplementary material Appendix 1 Fig. A6).

Model comparison

The hierarchical models, m_{opt} and m_{full}, predicted richness along the two novel transects dramatically better than did the multiple regression, m_{lm} (Fig. 4, Fig. 5). In predicting the observed FR richness for species common to SJ and FR transects, FR_{shared}, in the novel FR environmental conditions, m_{opt} decreased root mean squared error (RMSE) by 63% compared to m_{lm}, and m_{full} decreased RMSE by 28%. Likewise, in predicting both shared and novel species, FR_{all}, along the novel FR transects, m_{opt} and m_{full} decreased RMSE by 65 and 31%, respectively, compared to m_{lm}.

Discussion

The hierarchical model dramatically outperformed the multiple regression in predicting richness along two novel transects, and explicitly incorporates species-specific variation to construct community-level patterns. Ant richness in both mountain ranges peaked at middle elevations, and the patterns were best described by the distribution of species' thermal preferences with canopy cover moderating the local trap-scale richness. Congeners tended to respond to variables similarly, with little effect of deeper relationships. Species generally had low detectability even with long trapping bouts.

We did not assume the monotonic increase in richness with temperature typical of many richness studies (Pianka 1966, Kaspari et al. 2000, Allen et al. 2002, Sanders et al. 2007). Rather, we estimated species-level responses to temperature, a key benefit to the more complex model structure. In accordance with the well-established existence of thermal envelopes (Kaspari et al. 2015), we estimated a thermal optimum and breadth for each species. Under the phylogenetic niche conservatism hypothesis, the thermal breadth of each species would be most similar to that of its nearest relatives (Webb et al. 2002, Wiens and Donoghue 2004). In fact, genus explained a fair amount of the variation in ω_s and $b_{TempBreadth,s}$ (Supplementary material Appendix 1 Fig. A3; $\sigma^2_{among}/\sigma^2_{total}$: $\omega = 0.17$; $TempBreadth = 0.16$). Analyses of ants along elevational gradients in Costa Rica, the United States, Austria, and the Himalayas have documented high elevation phylogenetic clustering (Machac et al. 2011, Smith et al. 2014, Liu et al. 2018), consistent with the similarity in thermal preferences we detected among congeners. As richness patterns are direct products of species' elevational ranges, the distribution of thermal preferences has a large impact; our results suggest a strong effect of the evolutionary temperature preferences of a taxon – here at temperatures in the lower third of the gradient – diffused through some combination of selection and drift as species have diverged, on current richness patterns.

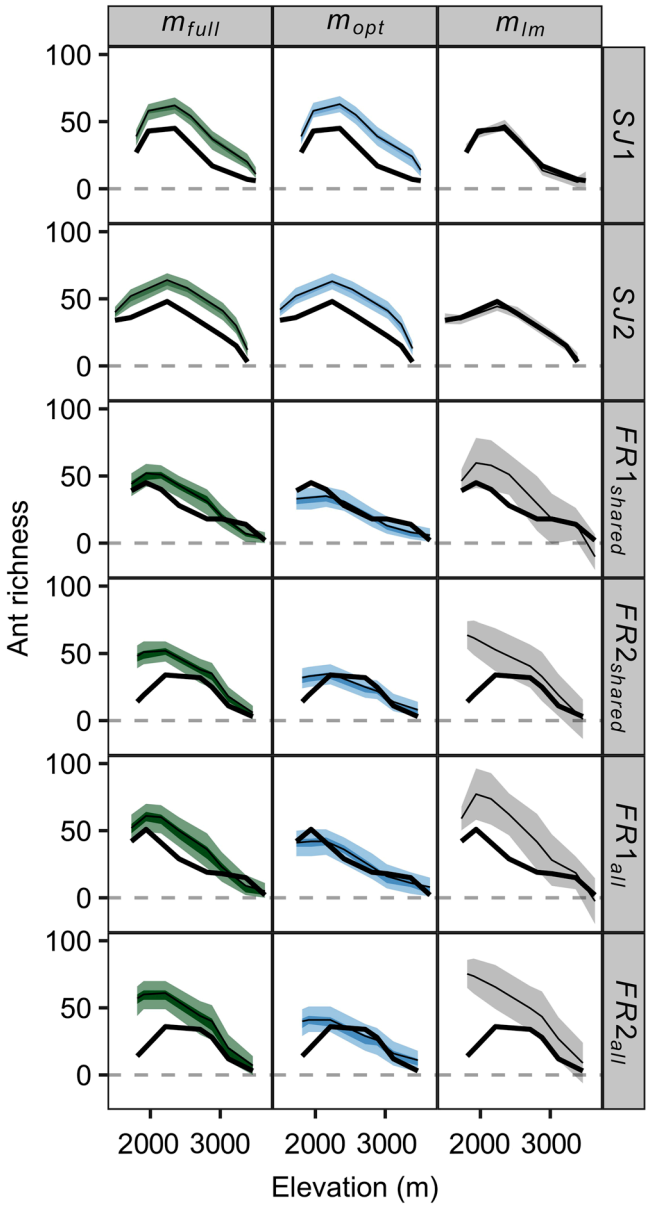

Figure 4. Predicted elevational richness patterns generated from the fit models. Interpolated richness (thick line) on each transect (rows) is shown with predictions by each model (columns): m_{full}, m_{opt}, and m_{lm} (thin line: median; dark band: 50% highest posterior density interval (HPDI); light band: 95% HPDI; m_{lm} band: 95% CI). All models estimated the San Juan transects well (*SJ*-1 and *SJ*-2). The Bayesian models (columns 1–2) estimated higher richness than was observed, accounting for undetected species. Using only species detected in both the San Juans and the Front Range and species-level (i.e. *b*) estimates, the Bayesian models (columns 1–2) predicted the observed richness pattern better than the multiple regression (column 3), though none fully captured the low richness observed along *FR*-2. Using all species in the Front Range with phylogenetically structured species-level responses drawn from the aggregate or genus (i.e. β or *B*) estimates, the median predicted richness showed a similar pattern, though with much higher uncertainty.

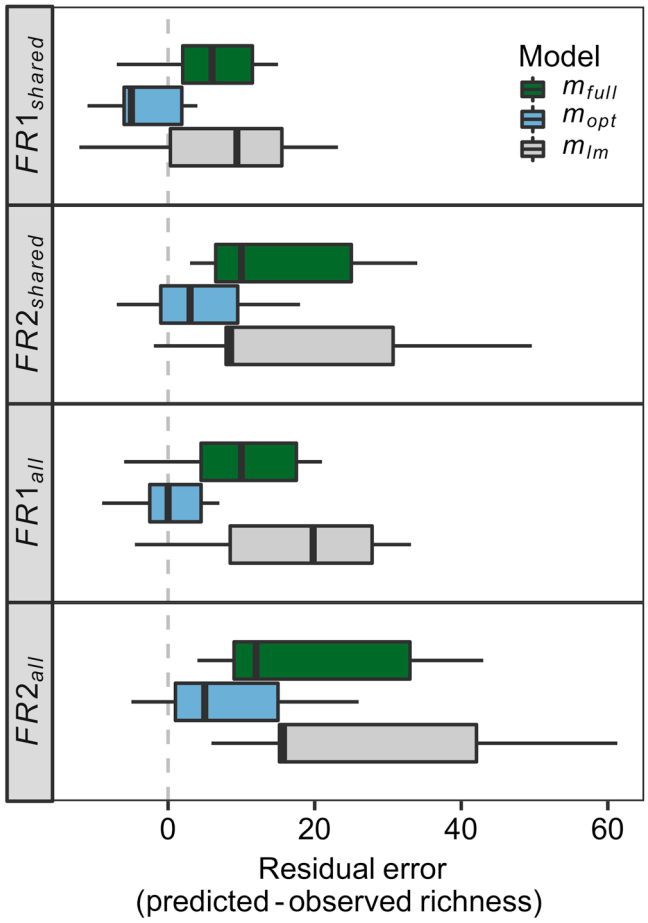

Figure 5. Boxplots of residual error in out-of-sample model predictions. Boxes show the distribution of residual error in the predicted richness and observed richness for each site on the novel transects. The multiple regression (m_{lm}: gray) tended to overestimate richness on both Front Range transects, both when fit with the shared species set among the Front Range and San Juans and when fit with all species. Additionally, the error was more variable among sites, indicated by the broader distributions. In contrast, both Bayesian models (m_{full}: green, m_{opt}: blue) predicted richness that was nearer to the observed values, with lower variation in error among sites.

Ant richness tended to decline with increased habitat complexity, as measured by canopy cover, possibly due to less effective chemical trails, less efficient travel, or less available heat, a deterrent to opportunistic or generalist ants (Hölldobler and Wilson 1990, Lassau and Hochuli 2004, Queiroz and Ribas 2016). However, the opposite has also been documented, attributed to abundant nesting and foraging sites (Andersen 1986, Pacheco and Vasconcelos 2012). Colorado, like most temperate ecosystems, lacks the diverse arboreal ant fauna common in the tropics, and so the negative effect of canopy cover on richness is perhaps unsurprising. Moreover, the largely coniferous forests do not produce the thick leaf litter that supports so many tropical ants (Fisher 1996, Longino and Colwell 2011), likely further limiting the utility of heavily forested habitats.

We found marginal support for an increase in ant richness with site-scale NPP, but no systematic variation of trap-scale richness with productivity. Productivity, or some climatic proxy, has been supported in other ant communities (Kaspari et al. 2000, Longino and Colwell 2011, Szewczyk and McCain 2016) as well as plants and vertebrates (Mittelbach et al. 2001, Hawkins et al. 2003, McCain 2007a, 2009). However, the relationship between productivity and species richness has been contentious (Mittelbach et al. 2001, Evans et al. 2005), with multiple proposed mechanisms and multiple empirical relationships. In ants, species density has been shown to increase with productivity (Kaspari et al. 2000), though most evidence involves large latitudinal spans (Kaspari et al. 2000, 2004), similar to the more regional, site-scale effects we detected. Additionally, pitfall traps are sensitive to ant activity levels (Bestelmeyer et al. 2000). If species density increases with local productivity, but activity decreases because resources are more accessible, pitfall traps may fail to detect any relationship. Manipulative experiments could disentangle these possibilities. Finally, we assumed consistent effects of trap-scale variables across the gradient, precluding the detection of local productivity effects that vary with elevation.

Many variables showed no relationship or were excluded from m_{opt}. Area had no detectible impact, in contrast to past analyses (Sanders 2002, Szewczyk and McCain 2016). The concurrent, opposing impacts of land cover and soil diversity in m_{full} lend support to the hypothesis that area summarizes such variables (Rosenzweig 1995), though as neither was in m_{opt}, any influence is minor. Likewise, tree density, understory vegetation biomass, and bare ground cover did not drive richness. While individual ant species or genera may respond to these local variables (Supplementary material Appendix 1 Fig. A3), their preferences negate one another, resulting in no aggregate impact.

In our explicitly top-down model, the aggregated effect of site-scale variables, scaled by ρ, determined the baseline for trap-scale occurrence. Estimates for ρ tended to be greater than 1 (Supplementary material Appendix 1 Table A3 and Fig. A6), suggesting strong site-scale effects on trap occupancy; a value of 0 would eliminate the term, indicating no impact. Additionally, site-scale occupancy probability described 75% of the variation in trap-scale occupancy probability in m_{opt} and 82% in m_{full}. Thus, the broader environment appears to drive local ant richness rather than local variation. Similarly, strong regional effects have been shown on local ant communities at a continental extent (Lessard et al. 2012). The dominance of site-scale effects is consistent with theoretical predictions as well, as the hyper-local positioning of ant colonies detected by pitfall traps is expected to be driven primarily by broader conditions (Hortal et al. 2010).

For the FR transects, the predicted richness intervals are much narrower when the b estimates are used directly, though this is only possible for species common to both mountain ranges (i.e. FR_{shared}). Nevertheless, a novel community can be predicted, given a regional species pool (i.e. FR_{all}). However, this requires generating species-level responses based on the fit genus-level responses, or based on the fit aggregate responses if the entire genus is novel. Further, a detectability probability must be drawn for each species. Thus, this additional stochasticity correspondingly increased the uncertainty (Fig. 4), though the median predictions of m_{opt} and m_{full} were quite close to the observed patterns for FR_{all} (Fig. 4, Fig. 5). The phylogenetic structure's flexibility in predicting richness in novel communities carries the cost of added noise. Nevertheless, the hierarchical model outperforms the clearly overfitted m_{lm} in predictive ability for similar but novel communities.

The data required to fit a complex model such as this necessitated several simplifying assumptions, highlighting areas for improvement in future efforts. First, we assumed that detection probability was constant for each species, though it could be allowed to vary across space or through time according to local conditions (Nichols et al. 2008, Kroll et al. 2015). Second, our sampling occurred across three years, with different sites and transects sampled each year (Supplementary material Appendix 1 Table A1). Incorporating an effect of sampling year may capture correlated interannual variation among species (Morris and Doak 2003, Bishop et al. 2014). Lastly, we relied on a genus-level phylogeny, assuming that the currently recognized taxonomy of each species was valid and that the relationships among genera were accurately reflected. However, our understanding of evolutionary relationships is continually improving (Brady et al. 2006, Moreau et al. 2006, Ward 2007, Ward et al. 2015, 2016), and inferences based on the phylogenetic component of our model should be considered provisional.

This model explicitly accounts for often unevaluated sources of uncertainty (Fisher 1996, Longino and Colwell 2011, Bharti et al. 2013). First, observations are samples from the true occupancy states, filtered through imperfect detection and sampling error (Fig. 1f–g). Second, the true occupancy state (i.e. z_{ijs} and Z_{is}) at each site or trap is probabilistic, representing one stochastic realization given the underlying occupancy probability (i.e. ψ_{ijs} and Ψ_{is}; Fig. 1b, d–e). The true richness pattern therefore varies stochastically even under identical occupancy probabilities. This is evidenced by differences over time (Bishop et al. 2014) or between adjacent transects where environmental conditions are similar (Grytnes 2003, Sanders et al. 2003). Third, occupancy probabilities depend on the environmental conditions and the species' or community's responses (Fig. 1a, c). The ultimate goal is to understand how and why these occupancy probabilities are shaped by environmental conditions and evolutionary history. These sources of uncertainty each undoubtedly contribute to the variation observed in elevational richness patterns (Grytnes 2003, Sanders et al. 2003, McCain 2007a, 2009, 2010, Szewczyk and McCain 2016) and hinder progress in understanding the factors that shape richness at this scale (Beck et al. 2012). Statistical methods (Colwell 2013) and repeated sampling (MacKenzie et al. 2002) can address the sampling and detection error of the first source of uncertainty

described above. However, only additional replication at the site- or transect-level can overcome the inherent stochasticity in the true occupancy states. This stochasticity is process error where true presences or absences depend on underlying occupancy probabilities, described above as the second source of uncertainty (Fig. 1b, d–g). The current true state, Z_{is}, is a single stochastic realization of a probabilistic process, and as such, replicated samples are required to improve the estimation of the underlying probabilities. For transect-level inference, transect-level replication across space or years will best capture this process error. Unfortunately, the substantial time and effort required make transect-level replication relatively uncommon (but see, Grytnes 2003, Sanders et al. 2003, Munyai and Foord 2012, Bishop et al. 2014).

Our hierarchical model allowed for an integrated evaluation of hypothesized richness drivers at two spatial scales while accounting for imperfect detection and phylogenetic effects. Further, species richness is conceptualized as an emergent property of the distribution of individual species, and is accordingly determined largely by the preferences and responses of each species. We found that the elevational richness of Colorado ants is driven by species-specific temperature preferences, local canopy cover, and site-scale NPP. The broader site-scale effects dominated, indicating a strong top-down influence on local trap-scale richness. Relationships among genera as incorporated here gave little information about responses to environmental variables, though congeners largely responded similarly. In addition to providing a much more detailed portrait of the community's responses to richness drivers, detectability estimates, and phylogenetic clustering, the more mechanistic, hierarchical model outperformed a simple multiple regression at predicting richness patterns in a novel mountain range, given a regional species pool. More complex statistical structures and transect-level replication, as implemented here, will allow for deep, robust insights into the processes that shape biodiversity.

Acknowledgements – We thank the members of the McCain lab, QDT, Maxwell Joseph, Kevin Bracy Knight, Helen McCreery, and two anonymous reviewers.
Funding – This study was funded by NSF (McCain: DEB 0949601), the CU Ecology and Evolutionary Biology Dept, and the CU Museum of Natural History.
Author contributions – CMM designed and funded the sampling. TMS identified specimens and developed the model. Both authors collected field data and contributed to the manuscript.

References

Allen, A. P. et al. 2002. Global biodiversity, biochemical kinetics, and the energetic-equivalence rule. – Science 297: 1545–1548.
Andersen, A. N. 1986. Diversity, seasonality and community organization of ants at adjacent heath and woodland sites in southeastern Australia. – Aust. J. Zool. 34: 53–64.
Beck, J. et al. 2012. What's on the horizon for macroecology? – Ecography 35: 673–683.
Bestelmeyer, B. T. et al. 2000. Field techniques for the study of ground-dwelling ants: an overview, description, and evaluation. – In: Agosti, D. et al. (eds), Ants: standard methods for measuring and monitoring biodiversity. Smithsonian Inst. Press, pp. 122–144.
Bharti, H. et al. 2013. Ant species richness, endemicity and functional groups, along an elevational gradient in the Himalayas. – Asian Myrmecol. 5: 79–101.
Bishop, T. R. et al. 2014. Elevation-diversity patterns through space and time: ant communities of the Maloti-Drakensberg Mountains of southern Africa. – J. Biogeogr. 41: 2256–2268.
Botes, A. et al. 2006. Ants, altitude and change in the northern Cape Floristic Region. – J. Biogeogr. 33: 71–90.
Brady, S. G. et al. 2006. Evaluating alternative hypotheses for the early evolution and diversification of ants. – Proc. Natl Acad. Sci. USA 103: 18172–18177.
Chao, A. and Jost, L. 2012. Coverage-based rarefaction and extrapolation: standardizing samples by completeness rather than size. – Ecology 93: 2533–2547.
Chao, A. et al. 2014. Rarefaction and extrapolation with Hill numbers: a framework for sampling and estimation in species diversity studies. – Ecol. Monogr. 84: 45–67.
Colwell, R. K. 2013. EstimateS: statistical estimation of species richness and shared species from samples. – Version 9.1.
Colwell, R. K. et al. 2012. Models and estimators linking individual-based and sample-based rarefaction, extrapolation and comparison of assemblages. – J. Plant Ecol. 5: 3–21.
Colwell, R. K. et al. 2016. Midpoint attractors and species richness: modelling the interaction between environmental drivers and geometric constraints. – Ecol. Lett. 19: 1009–1022.
Currie, D. J. et al. 2004. Predictions and tests of climate-based hypotheses of broad-scale variation in taxonomic richness. – Ecol. Lett. 7: 1121–1134.
Dennis, B. 1996. Should ecologists become Bayesians? – Ecol. Appl. 6: 1095–1103.
Ellison, A. M. 2004. Bayesian inference in ecology. – Ecol. Lett. 7: 509–520.
Evans, K. L. et al. 2005. Species–energy relationships at the macroecological scale: a review of the mechanisms. – Biol. Rev. 80: 1–25.
Fisher, B. L. 1996. Ant diversity patterns along an elevational gradient in the Réserve Naturelle Intégrale d'Andringitra, Madagascar. – Fieldiana Zool. 85: 93–108.
Gregg, R. E. 1963. The ants of Colorado. – Univ. of Colorado Press.
Grytnes, J. A. 2003. Species-richness patterns of vascular plants along seven altitudinal transects in Norway. – Ecography 26: 291–300.
Hadfield, J. D. and Nakagawa, S. 2010. General quantitative genetic methods for comparative biology: phylogenies, taxonomies and multi-trait models for continuous and categorical characters. – J. Evol. Biol. 23: 494–508.
Harrison, S. and Grace, J. B. 2007. Biogeographic affinity helps explain productivity–richness relationships at regional and local scales. – Am. Nat. 170: S5–S15.
Hawkins, B. A. et al. 2003. Energy, water, and broad-scale geographic patterns of species richness. – Ecology 84: 3105–3117.
Hölldobler, B. and Wilson, E. O. 1990. The ants. – Belknap Press of Harvard Univ. Press.

Hooten, M. B. and Hobbs, N. T. 2015. A guide to Bayesian model selection for ecologists. – Ecol. Monogr. 85: 3–28.
Hortal, J. et al. 2010. Understanding (insect) species distributions across spatial scales. – Ecography 33: 51–53.
Janzen, D. H. 1967. Why mountain passes are higher in the tropics. – Am. Nat. 101: 233–249.
Kaspari, M. et al. 2000. Energy, density, and constraints to species richness: ant assemblages along a productivity gradient. – Am. Nat. 155: 280–293.
Kaspari, M. et al. 2004. Energy gradients and the geographic distribution of local ant diversity. – Oecologia 140: 407–413.
Kaspari, M. et al. 2015. Thermal adaptation generates a diversity of thermal limits in a rainforest ant community. – Global Change Biol. 21: 1092–1102.
Kéry, M. and Royle, J. A. 2008. Hierarchical Bayes estimation of species richness and occupancy in spatially replicated surveys. – J. Appl. Ecol. 45: 589–598.
Kroll, A. J. et al. 2015. Evaluating multi-level models to test occupancy state responses of plethodontid salamanders. – PLoS One 10: e0142903.
Kumar, S. et al. 2017. TimeTree: a resource for timelines, timetrees, and divergence times. – Mol. Biol. Evol. 34: 1812–1819.
Laiolo, P. et al. 2018. Ecological and evolutionary drivers of the elevational gradient of diversity. – Ecol. Lett. <https://doi.org/10.1111/ele.12967>.
Lassau, S. A. and Hochuli, D. F. 2004. Effects of habitat complexity on ant assemblages. – Ecography 27: 157–164.
Lessard, J.-P. et al. 2012. Strong influence of regional species pools on continent-wide structuring of local communities. – Proc. R. Soc. B 279: 266–274.
Liu, C. et al. 2018. Mountain metacommunities: climate and spatial connectivity shape ant diversity in a complex landscape. – Ecography 41: 101–112.
Lomolino, M. 2001. Elevation gradients of species-density: historical and prospective views. – Global Ecol. Biogeogr. 10: 3–13.
Longino, J. T. and Colwell, R. K. 2011. Density compensation, species composition, and richness of ants on a neotropical elevational gradient. – Ecosphere 2: art29.
Longino, J. T. and Branstetter, M. G. 2018. The truncated bell: an enigmatic but pervasive elevational diversity pattern in Middle American ants. – Ecography doi:10.1111/ecog.03871
Machac, A. et al. 2011. Elevational gradients in phylogenetic structure of ant communities reveal the interplay of biotic and abiotic constraints on diversity. – Ecography 34: 364–371.
Mackay, W. P. and Mackay, E. E. 2002. The ants of New Mexico (Hymenoptera: Formicidae). – The Edwin Mellon Press.
MacKenzie, D. I. et al. 2002. Estimating site occupancy rates when detection probabilities are less than one. – Ecology 83: 2248–2255.
McCain, C. M. 2007a. Could temperature and water availability drive elevational species richness patterns? A global case study for bats. – Global Ecol. Biogeogr. 16: 1–13.
McCain, C. M. 2007b. Area and mammalian elevational diversity. – Ecology 88: 76–86.
McCain, C. M. 2009. Global analysis of bird elevational diversity. – Global Ecol. Biogeogr. 18: 346–360.
McCain, C. M. 2010. Global analysis of reptile elevational diversity. – Global Ecol. Biogeogr. 19: 541–553.
McGill, B. J. 2010. Matters of scale. – Science 328: 575–576.
Mittelbach, G. G. et al. 2001. What is the observed relationship between species richness and productivity? – Ecology 82: 2381–2396.
Mittelbach, G. G. et al. 2007. Evolution and the latitudinal diversity gradient: speciation, extinction and biogeography. – Ecol. Lett. 10: 315–331.
Moreau, C. S. and Bell, C. D. 2013. Testing the museum versus cradle tropical biological diversity hypothesis: phylogeny, diversification, and ancestral biogeographic range evolution of the ants. – Evolution 67: 2240–2257.
Moreau, C. S. et al. 2006. Phylogeny of the ants: diversification in the age of angiosperms. – Science 312: 101–104.
Morris, W. F. and Doak, D. F. 2003. Quantitative conservation biology: theory and practice of population viability analysis. – Sinauer Associates.
Munyai, T. C. and Foord, S. H. 2012. Ants on a mountain: spatial, environmental and habitat associations along an altitudinal transect in a centre of endemism. – J. Insect Conserv. 16: 677–695.
Nichols, J. D. et al. 2008. Multi-scale occupancy estimation and modelling using multiple detection methods. – J. Appl. Ecol. 45: 1321–1329.
Olson, D. M. 1994. The distribution of leaf litter invertebrates along a neotropical altitudinal gradient. – J. Trop. Ecol. 10: 129–150.
Pacheco, R. and Vasconcelos, H. L. 2012. Habitat diversity enhances ant diversity in a naturally heterogeneous Brazilian landscape. – Biodivers. Conserv. 21: 797–809.
Pagel, M. 1999. Inferring the historical patterns of biological evolution. – Nature 401: 877–884.
Pianka, E. R. 1966. Latitudinal gradients in species diversity: a review of concepts. – Am. Nat. 100: 33–46.
Queiroz, A. C. M. and Ribas, C. R. 2016. Canopy cover negatively affects arboreal ant species richness in a tropical open habitat. – Brazilian J. Biol. 1: 1–7.
Rahbek, C. 1995. The elevational gradient of species richness: a uniform pattern? – Ecography 18: 200–205.
Rosenzweig, M. L. 1995. Species diversity in space and time. – Cambridge Univ. Press.
Sabu, T. K. et al. 2008. Diversity of forest litter-inhabiting ants along elevations in the Wayanad region of the Western Ghats. – J. Insect Sci. 8: 1–14.
Samson, D. A. et al. 1997. Ant diversity and abundance along an elevational gradient in the Phillippines. – Biotropica 29: 349–363.
Sanders, N. J. 2002. Elevational gradients in ant species richness: area, geometry, and Rapoport's rule. – Ecography 25: 25–32.
Sanders, N. J. et al. 2003. Patterns of ant species richness along elevational gradients in an arid ecosystem. – Global Ecol. Biogeogr. 12: 93–102.
Sanders, N. J. et al. 2007. Temperature, but not productivity or geometry, predicts elevational diversity gradients in ants across spatial grains. – Global Ecol. Biogeogr. 16: 640–649.
Smith, M. A. 2015. Ants, elevation, phylogenetic diversity and community structure. – Ecosphere 6: art221.
Smith, M. A. et al. 2014. Diversity and phylogenetic community structure of ants along a Costa Rican elevational gradient. – Ecography 37: 720–731.
Stein, A. et al. 2014. Environmental heterogeneity as a universal driver of species richness across taxa, biomes and spatial scales. – Ecol. Lett. 17: 866–880.

Stevens, G. C. 1992. The elevational gradient in altitudinal range: an extension of Rapoport's latitudinal rule to altitude. – Am. Nat. 140: 893–911.
Szewczyk, T. M. and McCain, C. M. 2016. A systematic review of global drivers of ant elevational diversity. – PLoS One 11: e0155404.
Szewczyk, T. M. and McCain, C. M. 2018. Data from: Disentangling elevational richness: a multi-scale hierarchical Bayesian occupancy model of Colorado ant communities. – Dryad Digital Repository, <https://doi.org/10.5061/dryad.rt679ng>.
Terborgh, J. 1973. On the notion of favorableness in plant ecology. – Am. Nat. 107: 481–501.
Ward, P. S. 2007. Phylogeny, classification, and species-level taxonomy of ants (Hymenoptera: Formicidae). – Zootaxa 563: 549–563.
Ward, P. S. et al. 2015. The evolution of myrmicine ants: phylogeny and biogeography of a hyperdiverse ant clade (Hymenoptera: Formicidae). – Syst. Entomol. 40: 61–81.
Ward, P. S. et al. 2016. Phylogenetic classifications are informative, stable, and pragmatic: the case for monophyletic taxa. – Insectes Soc. 63: 489–492.
Webb, C. O. et al. 2002. Phylogenies and community ecology. – Annu. Rev. Ecol. Syst. 33: 475–505.
Wiens, J. J. and Donoghue, M. J. 2004. Historical biogeography, ecology and species richness. – Trends Ecol. Evol. 19: 639–644.

Supplementary material (Appendix ECOG-04115 at <www.ecography.org/appendix/ecog-04115>). Appendix 1–2.